ELSEVIER

Ceramics International 31 (2005) 1025–1029

CERAMICS
INTERNATIONAL

www.elsevier.com/locate/ceramint

Effects of chemical additives on high-field electromechanical properties of PMN–PT–BT ceramics

Yong S. Cho[a,*], Chang H. Yoon[b], Steven M. Pilgrim[b]

[a]*School of Advanced Materials Engineering, Yonsei University, 134 Shinchon-Dong, Seoul 120-749, South Korea*
[b]*New York State College of Ceramics at Alfred University, Alfred, NY 14802, USA*

Received 25 March 2004; received in revised form 22 April 2004; accepted 5 November 2004

Abstract

A chemical additive method using sol–gel reactions was used to modify the composition and resultant properties of a commercially available $0.96(0.91Pb(Mg_{1/3}Nb_{2/3})O_3–0.09PbTiO_3)–0.04\ BaTiO_3$ (PMN–PT–BT) ceramic. Without an additional ball-mixing process, several combinations of minor additives such as Fe, Ba, Sr, Zn, and Ti were incorporated by the chemical method. Weak- and high-field characteristics including dielectric properties, induced strain and polarization, and associated hystereses were evaluated for the samples sintered at 1200 °C for 4 h. All properties were found to depend on the chemical additives and temperature. Especially, the temperature dependence of high-field characteristics revealed different behavior from that reported for conventionally prepared samples. For example, the samples containing 0.5 wt.% SrO, 0.5 wt.% ZnO, and 0.5 wt.% TiO_2 did not exhibit a transition to piezoelectric behavior at the temperature expected from the dielectric measurements. Overall, the coating process has been successfully used to modify, and in some cases, enhance the high-field characteristics of PMN-based ceramics for electromechanical uses.

Keywords: A. Sol–gel processes; C. Dielectric properties; D. Niobates; E. Actuators

1. Introduction

$Pb(Mg_{1/3}Nb_{2/3})O_3$ (PMN) and related materials are well known for dielectric and electromechanical applications [1–6]. Several promising electromechanical properties like ~0.1% longitudinal strain (>0.03% transverse strain) at 1 MV/m and 0.1 Hz, and <0.05 tan δ at the temperature of peak weak-field permittivity T_{max} and 1 kHz have been reported [7,8]. These properties constitute enabling performance for a wide variety of military and commercial products.

The chemical modification method for incorporating sol–gel derived additives has been investigated to improve the performance of electronic ceramics [9–11]. Small amounts of the chemically-derived additives tend to coat particle surfaces of the calcined base materials at the nanoscale. Basically, they can contribute to homogeneity of the additive distribution over the sample after firing. They may also lead to more desirable microstructural characteristics, depending on the type of additives and base materials. The importance of the chemical additive method should be greater for more microstructure-sensitive materials such as barium titanates or ferrites [11,12]. In our previous work [13], this method was applied to a PMN-based relaxor composition, $0.96(0.91Pb(Mg_{1/3}Nb_{2/3})O_3–0.09PbTiO_3)–0.04\ BaTiO_3$, possessing 310 microstrain at 1 MV/m and 0.0029 tan δ at the temperature of peak weak-field permittivity T_{max} (~18,600 at 1 kHz). Several additives such as Sr, Ba, Ti, Zn, and Fe were selected for detailed study. The resultant high-field characteristics showed some abnormal behavior, which differs from the case of conventionally batch-mixed samples. This work explores the novel chemical additive method by using different sets of additives, with an emphasis on the temperature dependence of high-field characteristics.

---

* Corresponding author. Tel.: +82 2 2123 5848; fax: +82 2 365 5882.
E-mail address: yongscho@yonsei.ac.kr (Y.S. Cho).

0272-8842/$30.00 © 2004 Elsevier Ltd and Techna Group S.r.l. All rights reserved.
doi:10.1016/j.ceramint.2004.11.001

Table 1
Additive composition, bulk density and average grain size for the 0.96(0.91Pb($Mg_{1/3}Nb_{2/3}$)O_3–0.09PbTiO_3)–0.04 $BaTiO_3$ samples chemically-modified and sintered at 1200 °C for 4 h (theoretical density of the base composition ~8.00 g/cm^3)

Sample ID	Additive composition	Bulk density (g/cm^3)	Grain size (μm)
NO[a]	No additives	7.60	2.8
F5B5T5	0.5 wt.% Fe_2O_3, 0.5 wt.% BaO and 0.5 wt.% TiO_2	7.67	2.6
B5Z5T5	0.5 wt.% BaO, 0.5 wt.% ZnO and 0.5 wt.% TiO_2	7.61	3.8
S5Z5T5	0.5 wt.% SrO, 0.5 wt.% ZnO and 0.5 wt.% TiO_2	7.63	3.7

[a] [13].

Table 2
Dielectric properties measured at 1 kHz for the 0.96(0.91Pb($Mg_{1/3}Nb_{2/3}$)O_3–0.09PbTiO_3)–0.04 $BaTiO_3$

Sample ID	k' at RT	tan δ at RT	k'_{max}	tan δ at k'_{max}	Temperature at k'_{max}(°C)
NO[a]	18,600	0.029	18,600	0.029	25
F5B5T5	22,600	0.063	23,200	0.031	31
B5Z5T5	20,800	0.070	22,200	0.037	31
S5Z5T5	22,400	0.046	22,600	0.040	26

Samples sintered at 1200 °C for 4 h (RT: room temperature ~25 °C).
[a] Ref. [13].

2. Experimental procedure

A chemical method was used to modify a commercially-available PMN-based relaxor composition, 0.96(0.91Pb ($Mg_{1/3}Nb_{2/3}$)O_3–0.09PbTiO_3)–0.04 $BaTiO_3$ (Active Signal Technologies, MD, USA). The chemical method utilizes sol–gel reactions between the precursors of given additives such as Ti, Zn, Fe, Ba, and Sr. Table 1 represents the additive compositions and corresponding precursors, which were used in this work. An equal amount, 0.5 wt.% of each additive (in excess of the base PMN–PT–BT composition), was incorporated by the chemical method. Each additive composition was designated using the simple notation shown in Table 1. For example, F5B5T5 corresponds to a PMN–PT–BT sample containing 0.5 wt.% Fe_2O_3, 0.5 wt.% BaO, and 0.5 wt.% TiO_2.

The details of the chemical additive method are described in [13]. Titanium isopropoxide Ti[OCH(CH_3)$_2$]$_4$, zinc acetate dihydrate Zn(CH_3CO_2)$_2$·2H_2O, iron(III) acetylacetonate Fe[CH_3COOH=C(O–)CH_3]$_3$, barium acetate Ba(CH_3CO_2)$_2$, and strontium acetate Sr(CH_3CO_2)$_2$ were used as raw materials for the additives. After making a 0.063 M solution of titanium isopropoxide in isopropanol, Zn acetate or Fe acetylacetonate was dissolved in the solution. While stirring the solution, a catalytic amount of nitric acid was added. For the additives containing Ba and Sr, aqueous solutions of the Ba and Sr acetate (0.033 and 0.048 M, respectively) were separately prepared and then admixed with the previous cation-containing isopropanol solution. Gelation seemed to occur immediately. The base PMN–PT–BT powders were inserted into the gel solution. The resultant slurry was stirred at <60 °C until the solvent completely evaporated. The final powders containing the chemical additives were pressed at ~80 MPa to make disk-shaped pellets. The pressed pellets were sintered at 1200 °C for 4 h in a Pb atmosphere (formed by using a calcined PbZrO_3 + 5 wt.% ZrO_2 powder) after burn-out of organics at 600 °C for 2 h.

The sintered samples were characterized by fired density and grain size, which were obtained by the Archimedes' principle and the linear intercept method, respectively. For electrical measurement, the sintered pellets were electroded with a silver paste after sputtering both sides of the sample with Ag–Pd. Weak-field dielectric properties of the sintered samples were measured during cooling at 2 °C/min using an LCR meter (HP4284A) at several discrete frequencies (from 10 Hz to 1 MHz) and temperatures (from 170 to −20 °C). A modified Sawyer–Tower circuit was used to observe polarization behavior with electric field. In the case of longitudinal strain measurements, a Fotonic™ Sensor (MTI 2000 Fotonic Sensor) was used. The strain and polarization measurements were conducted simultaneously at 0.1 Hz with a change in temperature from 70 to −20 °C. The apparatus for the polarization and strain measurements included a multifunction synthesizer (HP8904A),

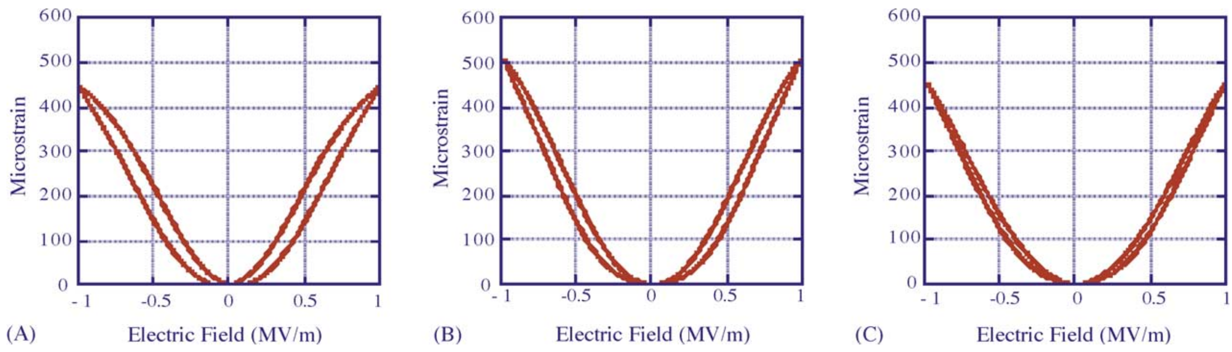

Fig. 1. Strain curves with electric field for the (A) F5B5T5, (B) B5Z5T5, and (C) S5Z5T5 samples.

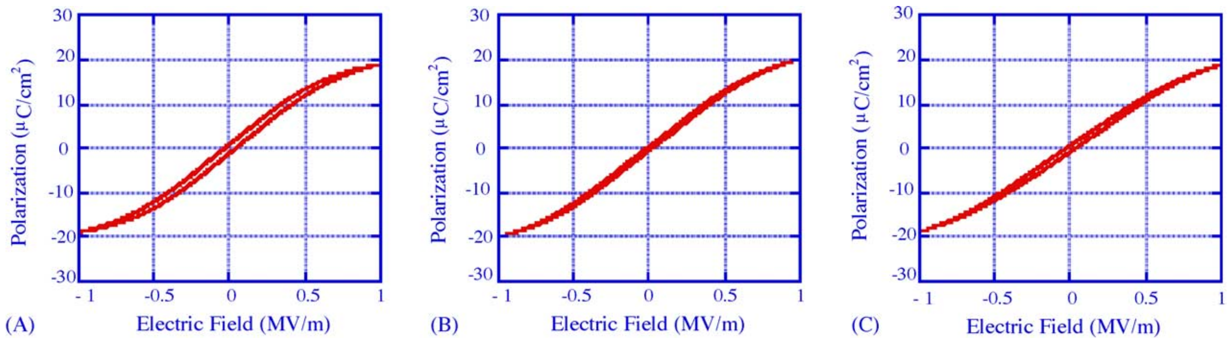

Fig. 2. Polarization curves with electric field for the (A) F5B5T5, (B) B5Z5T5, and (C) S5Z5T5 samples.

a high-voltage amplifier (Model 609D, Trek Co.) and an analog/digital converter (ADC488/85A) connected to a PC-all driven by LabView^{TM} computer routines.

3. Results and discussion

Weak-field dielectric properties of the PMN–PT–BT samples containing the chemical additives are summarized in Table 2. The properties correspond to the dielectric constant (k') and loss (tan δ) at room temperature, k'_{max}, tan δ at k'_{max} and T of k'_{max}, which were measured at 1 kHz. First, the significant increases in k'_{max} and k' at room temperature were observed by adding the chemical additives. This was accompanied with corresponding increases in tan δ and T of k'_{max}. This can be attributed to the increasing effects on the low-field dielectric properties, which resulted particularly from the incorporation of Fe and Zn. The substitution of Fe and Zn in the B^{I} site of the perovskite AB^{I}B^{II}O$_3$ structure (i.e., Mg site in Pb(Mg$_{1/3}$Nb$_{2/3}$)O$_3$) is likely to be responsible for the increase in k'. When considered the significant increase in k' by adding the chemical additives (for example, around 25% increase in the case of F5B5T5), however, it is believed that some other contributions exist beyond the effect of the ion substitution. The contributions are likely to be associated with the chemical processing and resultant microstructural characteristics. For example, a different grain size should be responsible for the dielectric properties. As shown in Table 1, grain size was found to apparently increase for the B5Z5T5 and S5Z5T5 samples. Our previous work [13] concluded that the addition of Fe, Zn and Ti increased the dielectric constant in spite of small contents when the same chemical method was used. In contrast, the addition of Ba and Sr engendered a decrease in k' and tan δ. When the additives having increasing and decreasing effect were combined, there should be compensating effects on the properties, which allow precise tailoring of the properties.

Figs. 1 and 2 show the polarization and strain curves as a function of electric field, measured at room temperature, 1 MV/m, and 0.1 Hz for the chemically-modified samples. The electromechanical parameters obtained from these curves are summarized in Table 3. Effective Q coefficient (Q_{eff}) was calculated by dividing the peak longitudinal strain (at ~1 MV/m) by the square of the peak polarization according to an equation of $\varepsilon = Q_{eff}\cdot\mathbf{P}^2$ where ε is the peak strain and $\mathbf{P}$ is the peak polarization. The simplification process and assumptions concerning the equation can be found in prior studies [14–16]. In addition, following ref. [8], the average hysteresis was determined using the response difference ($Y_{dec} - Y_{inc}$) between decreasing and increasing fields for the particular field (X) of interest. The sum of ($Y_{dec} - Y_{inc}$) normalized by the product of Y_{max} and the number of points is taken as the average hysteresis. Consequently, the product of average hysteresis, field range, and Y_{max} represents the piecewise-integrated area of the loop.

Compared to the base material, all other compositions exhibited significant increases in strain at an identical field. The highest longitudinal strain value of 0.051% was obtained for the B5Z5T5 sample. An increased T of k'_{max} appeared to result in higher polarization and peak saturation (at ~1 MV/m) as exemplified in all the samples containing chemical additives. As illustrated in Table 3, the chemically-modified samples exhibited increases in Q_{eff}. It is noticeable

Table 3
Electromechanical properties measured at 0.1 Hz and room temperature for the 0.96(0.91Pb(Mg$_{1/3}$Nb$_{2/3}$)O$_3$–0.09PbTiO$_3$)–0.04 BaTiO$_3$ samples sintered at 1200 °C for 4 h

Sample ID	Micro strain at 1 MV/m	Average strain hysteresis (%)	Polarization (μC/cm^2) at 1 MV/m	Average polarization hysteresis (%)	Q_{eff} ($\times 10^{-2}$ m4/C^2)
NO[a]	310	4.1	17	3.5	1.10
F5B5T5	440	9.6	19	6.2	1.22
B5Z5T5	510	6.6	20	2.7	1.25
S5Z5T5	460	5.4	19	2.7	1.41

[a] Ref. [13].

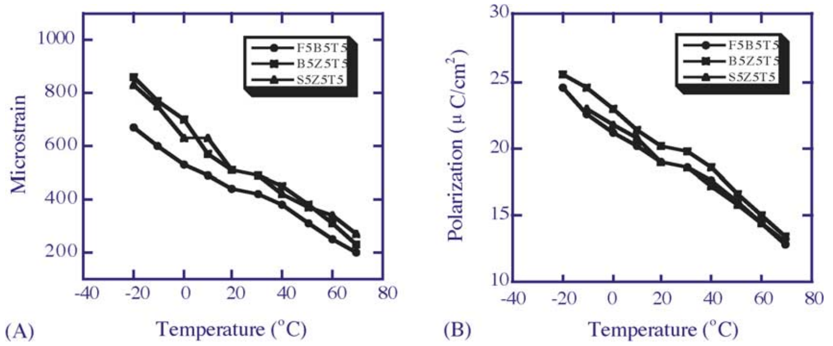

Fig. 3. Variations in (A) peak strain and (B) polarization with temperature for the chemically-modified samples.

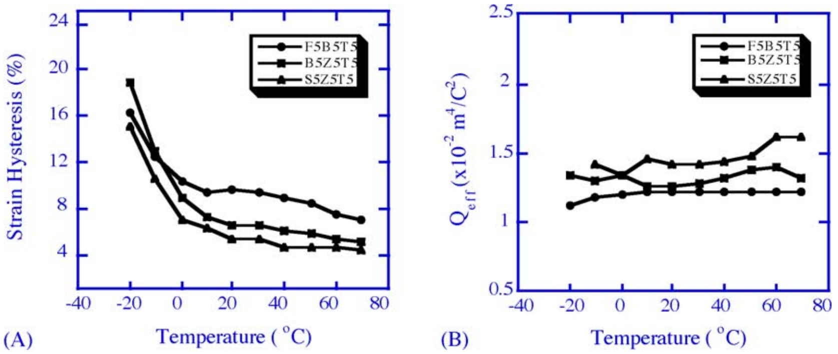

Fig. 4. Variations in (A) strain hysteresis and (B) Q_{eff} with temperature for the chemically-modified samples.

that S5Z5T5 has a high value of Q_{eff}, $1.41 \times 10^{-2}\ \mathrm{m^4/C^2}$. Table 3 also displays the calculated values of average hysteresis for strain and polarization measured at room temperature. As expected, all compositions exhibited low values, which are less than 10%.

Temperature dependence of the electromechanical properties was examined. Fig. 3 shows the changes in peak strain and polarization with temperature from 70 to −20 °C for the chemically-modified samples. The strain values tended to decrease with increasing temperature regardless of composition. The polarization behavior with temperature indicated the same trends with strain. Fig. 4 displays the variations in calculated average strain hysteresis and Q_{eff} with temperature for the compositions. As expected, the hysteresis also decreased with increasing temperature. The decreasing tendency of hysteresis was not significant above room temperature, particularly for the two compositions of B5Z5T5 and S5Z5T5. The S5Z5T5 sample exhibited the lowest hysteresis values over the temperature range. The resultant Q_{eff} was maintained unchanged over the temperature range. Only the S5Z5T5 tended to increase after around 50 °C.

The temperature dependence of the high-field characteristics is substantially different from previous bulk compositions. Pilgrim et al. [8,14] studied variations in transition temperature, which were obtained from the biased high-field characteristics such as strain, average hysteresis, polarization and Q_{eff} for bulk PMN–PT–BT compositions. According to the study, the high-field curves of Figs. 3 and 4 should demonstrate an abrupt change at a temperature correlated with the low-field transition. However, there are no dramatic changes in slope (corresponding to transition regions) of these curves. The temperature dependence of the electromechanical parameters clearly suggests that the electrically unbiased performances of the samples are consistent with primarily paraelectric response over the temperature range.

4. Conclusions

The chemical additive method was successfully used to modify the low- and high-field properties of the PMN–PT–BT-based ceramics for electromechanical uses. Even small levels of additives such as Fe, Sr, Ba, Zn, and Ti changed the properties significantly. This result was unpredicted from the literature on conventionally-processed samples. Particularly, the variations in high-field parameters with temperature demonstrated significant differences. In the case of the chemical method, the distinctive slope changes in high-field curves were not found around the transition temperature obtained from the low-field dielectric properties. Although the reason(s) are unclear, chemical processing can partially decouple the high-field electromechanical properties from the low-field properties. This is accompanied by improved performance across a wide temperature range.

Acknowledgment

This work was supported by the Office of Naval Research under contract no. N00014-97-C-0285.

References

[1] L.E. Cross, Relaxor ferroelectrics, Ferroelectrics 76 (1987) 241–267.

[2] S. Nomura, K. Uchino, Electrostrictive effect in $Pb(Mg_{1/3}Nb_{2/3})O_3$-type materials, Ferroelectrics 41 (1982) 117–132.

[3] K.M. Rittenmyer, Electrostrictive ceramics for underwater transducer applications, J. Acoust. Soc. Am. 95 (2) (1994) 849–856.

[4] Q. Zhang, W. Pan, A. Bhalla, L.E. Cross, Electrostrictive and dielectric response in lead magnesium niobate–lead titanate (0.9PMN·0.9PT) and lead lanthanum zirconate titanate (PLZT 9.5/65/35) under variation of temperature and electric field, J. Am. Ceram. Soc. 72 (4) (1989) 599–604.

[5] K. Uchino, L.E. Cross, S. Nomura, Inverse hysteresis of field induced elastic deformation in the solid solution 90 mol% $Pb(Mg_{1/3}Nb_{2/3})O_3$–10 mol% $PbTiO_3$, J. Mater. Sci. 15 (1980) 2643–2646.

[6] S. Chen, S. Cheng, C. Wang, Effect of barium titanate on microstructural evolution and properties of lead zinc magnesium niobate ceramics, J. Am. Ceram. Soc. 74 (2) (1991) 400–405.

[7] M. Massuda, K. Bridger, J.D. Prodey, S.M. Pilgrim, High-field electromechanical properties of some PMN–Pt-based relaxors, Ferroelectrics 158 (1994) 337–342.

[8] M. Pilgrim, M. Massuda, J.D. Prodey, A.P. Ritter, Electromechanical properties of some $Pb(Mg_{1/3}Nb_{2/3})O_3$–$PbTiO_3$–$(Ba,Sr)TiO_3$ ceramics: I, J. Am. Ceram. Soc. 75 (7) (1992) 1964–1969.

[9] Y.S. Cho, V.R.W. Amarakoon, Nanoscale coating of silicon and manganese on ferrimagnetic yttrium iron garnets, J. Am. Ceram. Soc. 79 (1996) 2755–2758.

[10] J.G. Fagan, V.R.W. Amarakoon, Sol–gel coating of $YBa_2Cu_3O_{7-x}$ with TiO_2 for enhanced anisotropic grain growth, J. Mater. Res. 8 (1993) 1501–1509.

[11] F.A. Selmi, V.R.W. Amarakoon, Sol–gel coating of powders for processing electronic ceramics, J. Am. Ceram. Soc. 71 (1988) 934–937.

[12] Y.S. Cho, V.L. Burdick, V.R.W. Amarakoon, Enhanced microwave magnetic properties in nonstoichiometric yttrium iron garnets for high power applications, IEEE Trans. Magn. 34 (1998) 1387–1389.

[13] Y.S. Cho, S.M. Pilgrim, H. Giesche, K. Bridger, Dielectric and electromechanical properties of chemically-modified PMN–PT–BT ceramics, J. Am. Ceram. Soc. 83 (10) (2000) 2473–2480.

[14] S.M. Pilgrim, M. Massuda, A.E. Sutherland, Electromechanical determination of the high-field phase transition of $Pb(Mg_{1/3}Nb_{2/3})O_3$–$PbTiO_3$–$(Ba,Sr)TiO_3$ relaxor ferroelectrics, J. Am. Ceram. Soc. 75 (7) (1992) 1970–1974.

[15] U. Kumar, L.E. Cross, A. Halliyal, Pyroelectric and electrostrictive properties of $(1 - x - y)$PZN·xBT·yPT ceramic solid solutions, J. Am. Ceram. Soc. 75 (8) (1992) 2155–2164.

[16] S.M. Pilgrim, M. Massuda, J.D. Prodey, Electromechanical properties of some $Pb(Mg_{1/3}Nb_{2/3})O_3$–$PbTiO_3$–$(Ba,Sr)TiO_3$ ceramics: Part two, J. Am. Ceram. Soc. 7 (8) (1995) 1501–1509.